JOURNAL OF SOLID STATE CHEMISTRY 35, 181–186 (1980)

The Crystal Structure and Stability of $Ba_5Fe_4S_{11}$

S. COHEN, N. KIMIZUKA,* AND H. STEINFINK

Materials Science and Engineering, Department of Chemical Engineering, The University of Texas, Austin, Texas 78712

Received October 29, 1979

The crystal structure of $Ba_5Fe_4S_{11}$ is orthorhombic, a = 16.060(1) Å, b = 7.260(1) Å, c = 8.863(1) Å, Z = 2, $Pmn2_1$. The structure was solved from a three-dimensional analysis using 1452 reflections with intensities $I \geq 2\sigma(I)$. The refinement converged to R = 0.0204, wR = 0.0216. The structure consists of BaS_6 distorted trigonal prisms and an irregular BaS_7 pentagonal bipyramid which articulate into a three-dimensional framework enclosing a cavity which contains the tetranuclear unit Fe_4S_{11}. The four FeS_4 tetrahedra form an isolated cluster in which a central tetrahedron shares one edge with another tetrahedron and the two remaining corners with two additional tetrahedra. The phase is stable below 750°C although the kinetics for formation are slow.

Introduction

In an attempt to prepare $Ba_3Fe_2S_5$, which is one of the end members in the $Ba_3Fe_{1+x}S_5$ series (*1*), mixtures of 3BaS:2Fe and various amounts of S were introduced into graphite ampules and sealed in evacuated Vycor tubes. Reaction was usally carried out for 24 hr at 900–1000°C, after which the product was slowly cooled to room temperature. Powder patterns of a 3BaS:2Fe:4S mixture reacted at 1000°C showed the presence of a new phase which was eventually shown to be $Ba_5Fe_4S_{11}$. Its crystal structure and stability range are described in this communication.

Experimental

A black single crystal measuring 0.05 × 0.10 × 0.20 mm was selected from the reaction product and used for all subsequent X-ray diffraction analyses. Weissenberg and Buerger precession photographs showed diffraction symmetry *mmm*, with systematic absences $h0l$, $h + l = 2n + 1$ consistent with space groups $Pmnm$ and $Pmn2_1$. Lattice constants were determined from a least-squares refinement of 2θ measurements at room temperature of 30 intense reflections between 25 and 30° using a Syntex $P2_1$ autodiffractometer and graphite monochromatized Mo$K\alpha$ radiation. The lattice constants are a = 16.060(1), b = 7.260(1), c = 8.863(1) Å (λ = 0.71069 Å). Intensity data were collected to sin θ/λ = 0.70. A total of 1649 independent reflections was measured by the ω-scan technique at rates varying from 1.5 to 5.0° min^{-1}, such that the less intense reflections were scanned for a longer interval. Background intensities were counted on each side of the peak at one-half the peak scan

* Permanent address: National Institute for Researches in Inorganic Materials, 1-1, Namiki, Sakuramura, Niihari-Gun, Ibaraki, Japan 300-31.

0022-4596/80/140181-06$02.00/0

time and at positions offset by $\omega = \pm 1°$ from the peak. Four reflections were monitored 19 times during the data collection process and no significant intensity fluctuations were observed. The standard deviations for the intensities were calculated from the expressions $\sigma(I) = [S^2(CT + B_1 + B_2) + (pI)^2]^{1/2}$, where S is the scan rate, CT is the total integrated count, B_1 and B_2 are background counts, and the intensity is $I = S[CT - (B_1 + B_2)]$. The parameter p was set equal to 0. A total of 1452 reflections with intensities $I \geqq 2\sigma(I)$ was used in the subsequent calculations which led to the structure determination and its refinement. Intensities were transformed into a set of structure amplitudes after making Lorentz, polarization (including those due to the incident beam monochromator), and absorption corrections ($\mu_l = 134.6$ cm^{-1}). The latter were obtained by approximations of the shape of the crystal by six faces and the corrections varied from 3.263 to 1.837.

Structure Determination

A statistical analysis made on 200 normalized structure amplitudes showed that the structure is acentric, implying that the space group is $Pmn2_1$. The direct method employing the program MULTAN was used to calculate phases for the initial electron density map which yielded the special position of Ba1. The origin was fixed by arbitrarily choosing $z = \frac{1}{4}$ for the z parameter of that ion. A three-dimensional Patterson vector map revealed the general locations of the other two Ba ions. Phases based on these positions and used in the calculations of the next Fourier map provided the locations of the other ions. Full-matrix least-squares refinement using the program NUCLS, converged to $R = 0.0258$ and $wR = 0.0231$ for all 1649 reflections, and $R = 0.0204$ and $wR = 0.0216$ for the 1452 observed reflections [$(R = \Sigma\big||F_o| - |F_c|\big|/\Sigma|F_o|$, $wR = (\Sigma w(|F_o| - |F_c|)^2/\Sigma wF_o^2)^{1/2}$, $w = \sigma(|F_o|)^{-2}$]. The standard deviation for an observation of unit weight was 1.16; the extinction coefficient was 2.77×10^{-7}. The atomic scattering factors for Ba, Fe, and S and the corrections for the real and imaginary parts of dispersion were taken from Ref. (*2*). The final difference electron density map showed random peaks scattered about the unit cell with a maximum of 0.8 e Å^{-3}. Table I lists the final positional and thermal parameters for the structure and Table II contains observed and calculated structure amplutides.[1]

Discussion

Table III contains a listing of bond distances and angles of interest in this structure. The S–S distances are shown for values less than 4 Å. Figure 1 is a stereoscopic view of the structure seen along the c axis.

Ba2 is coordinated to nine sulfur ions which form a capped, distorted trigonal prism. S4–S6–S3 and S3–S7–S4 form the two triangular faces and the S–S distances are those shown in Table III. However, the height of the prism is 4.919 Å for S3–S4 and 5.80 Å for S6–S7. The three rectangular faces are capped by S5, S6, and S2. The next Ba2 prism, along the c axis, shares the S3–S4 edge and S6 completes its triangular face so that a zig-zag chain of prisms exists parallel to c. The coordination polyhedron around Ba3 can be described in terms of a distorted trigonal prism formed by two tri-

[1] See NAPS Document No. 03645 for 18 pages of supplementary material. Order from NAPS c/o Microfiche Publications, P.O. Box 3513, Grand Central Station, New York, N.Y. 10017. Remit in advance, in U.S. funds only $5.00 for photocopies or $3.00 for microfiche. Outside the United States and Canada, postage is $3.00 for a photocopy or $1.50 for a fiche.

TABLE I

ATOMIC PARAMETERS AND THEIR STANDARD DEVIATIONS ($\times 10^4$)[a]

	x	y	z	β_{11}	β_{22}	β_{33}	β_{12}	β_{13}	β_{23}
Ba1	½	290(1)	¼	17(0)	128(1)	25(1)	—	—	3(1)
Ba2	6718(0)	5255(1)	4901(1)	14(0)	80(1)	33(0)	−2(0)	0(0)	1(1)
Ba3	8036(0)	193(1)	3728(1)	11(0)	72(1)	31(0)	−1(0)	−1(0)	−6(1)
Fe1	½	425(2)	6362(2)	9(0)	72(3)	21(1)	—	—	−3(2)
Fe2	½	3843(2)	7971(2)	11(0)	64(3)	32(2)	—	—	−4(2)
Fe3	1169(1)	4781(1)	5994(1)	11(0)	53(2)	28(1)	2(1)	−1(0)	0(0)
S1	½	876(4)	8901(3)	12(1)	78(4)	24(2)	—	—	−1(3)
S2	½	3385(4)	5480(3)	15(1)	70(5)	25(3)	—	—	8(3)
S3	3272(1)	2550(3)	1791(3)	15(1)	57(3)	49(2)	−3(1)	4(1)	6(2)
S4	2031(1)	2536(3)	6716(2)	22(1)	60(3)	34(2)	17(1)	−4(1)	−1(2)
S5	1178(1)	646(3)	407(2)	12(1)	107(4)	37(2)	−13(1)	−1(1)	9(2)
S6	1190(1)	4608(3)	3451(2)	18(1)	141(4)	28(2)	23(1)	0(1)	2(2)
S7	0	4163(4)	7279(3)	9(1)	141(6)	46(3)	—	—	2(3)

[a] The temperature factor is exp [$-(\beta_{11}h^2 + \beta_{22}k^2 + \beta_{33}l^2 + 2\beta_{12}hk + 2\beta_{13}hl + 2\beta_{23}kl)$].

angular faces S1, S3, S4 and S3, S4, S5 with S6 and S5 capping two rectangular faces. It can also be visualized as an orthorhombic bipyramid formed by S3, S4, and S5. The longest edge is S3–S4, 4.919 Å, and is shared with the Ba2 prism. The triangular face S3–S4–S5 is shared with the next bipyramid so that a column parallel to c exists. The columns, separated by the b-axis periodicity, are then connected by the Ba2 prisms through the S3–S4 edges, which are the height of the prism, into two-dimensional layers parallel to the (100) planes. These slabs are bridged along the a axis by Ba1, which is situated in the mirror planes at $x = 0$ and ½. It is coordinated to seven sulfur ions which form an irregular pentagonal bipyramid. The tetranuclear FeS_4 units also serve to connect the slabs to complete the three-dimensional framework of the structure.

The tetranuclear FeS_4 units consist of two tetrahedra, around Fe1 and Fe2, sharing the S1–S2 edge and in turn sharing a corner at S6 with two tetrahedra around Fe3, the latter being connected by corner sharing at S7. These units are isolated from each other and repeat with the b-axis peri-

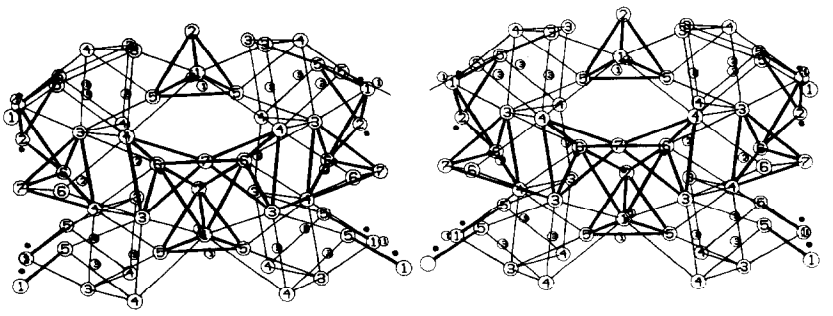

FIG. 1. Stereoscopic view of $Ba_5Fe_4S_{11}$. The large circles represent S, smaller circles Ba, and solid circles Fe. The numbers correspond to the atom labeling of Table I. The a axis is horizontal, the b axis is vertical, and the height is $1.4c$. The heavy lines outline the tetranuclear cluster Fe_4S_{11}.

TABLE III

BOND DISTANCES AND ANGLES[a]

Distances (Å)

Ba1–	S1	3.218(3)	Fe1–	S1	2.275(3)	S4 –	S5 3.803(3)
	S2	3.468(2)		S2	2.286(3)		S5 3.867(3)
	2S3	3.286(2)		2S5	2.215(2)		S6 3.530(3)
	2S5	3.269(2)	Fe2–	S1	2.307(3)		S6 3.851(3)
	S7	3.240(3)		S2	2.233(3)		S7 3.505(2)
Ba2–	S3	3.385(2)		2S6	2.259(2)	S5 –	S5 3.786(2)
	S3	3.402(2)	Fe3–	S3	2.250(2)		S6 3.944(3)
	S4	3.244(2)		S4	2.232(2)	S6 –	S6 3.823(3)
	S4	3.286(2)		S6	2.258(2)		S7 3.908(2)
	S6	3.261(2)		S7	2.242(1)	Fe1–Fe2	2.862(2)
	S7	3.632(0)	S1–	S2	3.537(4)	Fe2–Fe3	3.421(1)
	S2	3.118(0)		2S5	3.794(2)	Fe3–Fe3	3.756(1)
	S5	3.132(2)		2S6	3.817(2)		
	S6	3.628(2)		2S3	3.968(2)		
Ba3–	S3	3.208(2)	S2–	2S5	3.486(2)		
	S3	3.389(2)		2S6	3.566(2)		
	S4	3.150(2)		S7	3.350(4)		
	S4	3.116(2)	S3–	S4	3.601(3)		
	S5	3.220(2)		S4	3.725(3)		
	S5	3.389(2)		S5	3.857(3)		
	S1	3.252(0)		S6	3.711(3)		
	S6	3.447(2)		S7	3.686(2)		

Angles (°)

S1–Fe1–S2	101.7(1)	S3–Fe3–S7	110.3(1)
S5–Fe1–S5	117.5(1)	S3–Fe3–S6	110.8(1)
2S5–Fe1–S2	101.5(1)	S3–Fe3–S4	106.9(1)
2S5–Fe1–S1	115.4(0)	S7–Fe3–S6	120.6(1)
S6–Fe2–S6	115.6(1)	S7–Fe3–S4	103.2(1)
2S6–Fe2–S2	105.1(0)	S6–Fe3–S4	103.7(1)
2S6–Fe2–S1	113.4(1)		
S1–Fe2–S2	102.4(1)		

[a] Standard deviations in parentheses.

odicity. The Fe1–Fe2 distance is short, as expected for edge-sharing tetrahedra. A tetranuclear unit of FeS_4 tetrahedra has been previously observed in $Ba_6Fe_8S_{15}$ (*3*) but they share corners only and are part of an infinite, one-dimensional column.

The formal valence of iron in $Ba_5Fe_4S_{11}$ is +3. Sulfides containing trivalent iron in a tetrahedral environment are difficult to prepare (*4*). The alkali iron sulfides $AFeS_2$ (*A* = K, Rb, Cs) (*5*) have weak, temperature-independent paramagnetism (*6*) and it is doubtful that Fe can be considered trivalent. In $KFeS_2$ ESR measurements yield values for the *g* tensor of Fe^{3+} which indicate a sulfur orbital contribution (*7*). The formally trivalent iron compounds in the Ba–Fe–S system which have been previously described, α- and β-$Ba_9Fe_4S_{15}$ (*1*) and $Ba_4Fe_2S_6$ $[S_{2/3}(S_2)_{1/3}]$ (*8*), also show the presence of intermediate valence states. $BaFe_2S_4$, the end member of the infinitely adaptive series $Ba_{1+x}Fe_2S_4$, is synthesized at a sulfur vapor pressure of about 7 atm and 800°C and Ba_3FeS_5 is also a high-pressure phase in agreement with the well-

known effect that high-pressure stabilizes higher valence, (*10*).

The application of the equations to the calculation of valence and Mössbauer isomer shifts (*9*) for the three crystallographically independent iron atoms yields the values Fe1 = +2.88, δ = 0.25 mm/sec; Fe2 = +2.74, δ = 0.31 mm/sec; Fe3 = +2.89, δ = 0.24 mm/sec. The intermediate valence states can be realized by back donation of electrons from the S^{2-}:$3p^6$ valence band into the Fe^{3+}:$3d^6$ band (*4*). The sharing of one edge by two tetrahedra implies the formation of a three-electron bond with the Fe b_{1g} orbitals or the creation of 0.09 holes per S in the valence band of the cluster (*4*). If the electron is localized in the Fe1–Fe2 bond then a charge distribution Fe1 = Fe2 = +2.5 and 2Fe3 = +3 would be expected for the cluster. The calculated distribution, obtained from the Fe–S distances, shows that Fe2 has retained the highest electron density and Fe1 and Fe3 are equivalent. Also, only 0.6 electron has been back donated or about 0.05 hole/S exists in the S^{2-}:$3p^6$ band of the cluster. Fe2 shares an edge with Fe1 and the usual short distance is observed. Fe2–2Fe3 is 3.42 Å because of corner sharing, and Fe1 is isolated from Fe3, the distance being 6.93 Å. The central Fe2 has, thus, a distinctly different environment and would be expected to have an isomer shift different from that of the other iron atoms. The delocalization of 0.6 electron over the three distances Fe2–Fe1 and Fe2–2Fe3 would produce a resultant charge distribution of Fe2 = +2.7 and Fe1 = 2Fe3 = +2.9. Spectroscopic data for this compound (*XPS*, *UPS*, and XES) and comparison with an $X\alpha$ calculation could check whether such a postulated electron distribution is correct.

The initial discovery of $Ba_5Fe_4S_{11}$ was a result of attempts to synthesize a different phase. After the stoichiometry of the compound was known its stability range was investigated. BaS, FeS (troilite), and FeS_2 (pyrite) were used as starting materials in the ratio 5:2:2. The mixture was placed into a closed graphite tube which in turn was sealed in an evacuated Vycor ampule. Prior to being sealed, the tube was filled with Vycor glass powder to eliminate dead space (*11*). The FeS and FeS_2 were synthesized from the elements by a solid-state reaction in evacuated Vycor tubes. Concurrently with these experiments we also used as starting materials BaS, Fe, and S in the ratio 5:4:6 and they were subjected to a treatment identical to that used for the other starting compounds. At the end of the reaction the samples were quenched in either water or air. The identical phases were always observed. The X-ray powder diffraction technique, using a diffractometer equipped with a diffracted beam monochromator and Cu$K\alpha$ radiation, was used to identify the phases. Table IV lists the results obtained for the various experimental conditions.

$Ba_5Fe_4S_{11}$ does not form at 750°C or higher temperatures. At 700°C and below the three phases shown in Table IV were observed. It is evident that equilibrium could not be reached.

To study the reaction rate at 550°C about

TABLE IV

PHASE OBTAINED FROM THE REACTION MIXTURE 5BaS:2FeS:2FeS_2

Temp. (°C)	Phases	Reaction time (day)
1000	α-9-4-15,[a] "1-2-4"[b]	1
900	α-9-4-15, "1-2-4"	2
800	α-9-4-15, "1-2-4"	2
750	α-9-4-5, "1-2-4"	8
700	α-9-4-15, 5-4-11, "1-2-4"	3
650	α-9-4-15, 5-4-11, "1-2-4"	10
550	α-9-4-15, 5-4-11, "1-2-4"	30

[a] The numerals *A-B-C* stand for $Ba_AFe_BS_C$.

[b] "1-2-4" indicates that the observed phase was part of the infinitely adaptive series $Ba_{1+x}Fe_2S_4$.

20 g of a 5BaS, 2FeS, and $2FeS_2$ mixture was reacted in an evacuated Vycor tube without a graphite crucible because no chemical reaction occurs between the mixture and the container at this low temperature. In intervals of about 5 days the tube was air quenched and about 100 mg of sample withdrawn and analyzed; then the sample was returned to the reaction tube, which was evacuated and resealed, and the reaction was continued. After 5 days the reaction product displayed a pattern with very broad diffraction profiles. As the reaction time increased α-$Ba_9Fe_4S_{15}$ and one of the phases in the $Ba_{1+x}Fe_2S_4$ series appeared although the crystallinity was poor. After about 20 days diffraction lines ascribable to $Ba_5Fe_4S_{11}$ began to appear and its concentration had increased somewhat when the experiment was terminated. It was evident that the kinetics for the formation of $Ba_5Fe_4S_{11}$ are very slow. This conclusion is further reinforced by the results at 650 and 700°C. The reaction products at these temperatures were always unconsolidated powders, with the crystallinity improving with increasing temperature. The reaction products at 750°C and above are very well sintered into cylindrical shapes. At 743°C, FeS_2 decomposes into FeS and a liquid (*12*) and the reaction kinetics become fast. No evidence of $Ba_5Fe_4S_{11}$ is seen at 750°C or higher temperatures. We suggest that $Ba_5Fe_4S_{11}$ probably decomposes at a temperature above 750°C and that single-phase material cannot be prepared at lower temperatures because the reaction kinetics are too slow. It is probable that in a suitable flux single-phase $Ba_5Fe_4S_{11}$ could be obtained.

It is now possible to explain the formation of $Ba_5Fe_4S_{11}$ in the original experiment. The BaS : Fe ratio of 3 : 2 provides the stoichiometric amounts required for formation. The reaction at 1000°C inhibits the formation of this phase but during the slow cooling process equilibration in the system begins and the formation of $Ba_5Fe_4S_{11}$ is initiated.

Acknowledgments

The authors gratefully acknowledge the research support of the National Science Foundation under Grant DMR76-82092 and of the Robert A. Welch Foundation, Houston, Texas.

References

1. S. COHEN, L. E. RENDON-DIAZMIRON, AND H. STEINFINK, *J. Solid State Chem.* **25,** 179 (1978).
2. "International Tables for X-Ray Crystallography" (J. A. Ibers and W. C. Hamilton, Eds.), Vol. IV, Tables 2.2A, 2.3.1, Kynoch Press, Birmingham (1974).
3. H. Y. HONG AND H. STEINFINK, *J. Solid State Chem.* **5,** 93 (1972).
4. J. B. GOODENOUGH, *Mater. Res. Bull.* **13,** 1305 (1978).
5. W. BRONGER, "Crystallography and Crystal Chemistry with Layered Structures" (F. Levy, Ed.), Reidel, Dordrecht (1976).
6. W. BRONGER, *Z. Anorg. Allg. Chem.* **359,** 225 (1968).
7. W. V. SWEENEY AND R. E. COFFMAN, *Biochim. Biophys. Acta* **286,** 26 (1972).
8. J. T. HOGGINS, L. E. RENDON-DIAZMIRON, AND H. STEINFINK, *J. Solid State Chem.* **21,** 79 (1977).
9. J. T. HOGGINS AND H. STEINFINK, *Inorg. Chem.* **15,** 1682 (1976).
10. J. S. SWINNEA AND H. STEINFINK, *J. Solid State Chem.* **32,** 329 (1980).
11. G. KULLERUD, *in* "Research Techniques for High Pressure and High Temperature" (G. C. Ulmer, Ed.), Springer-Verlag, New York (1971).
12. G. KULLERUD, *in* "The Interpretation of Geological Phase Diagrams" (E. G. Ehlers, Ed.), Freeman, San Francisco (1972).